

## Deuterium Isotope Effects in A:T and A:U Base Pairs: A Computational NMR Study

Pietro Vidossich,<sup>†,§</sup> Stefano Piana,<sup>‡</sup> Andrea Miani,<sup>†</sup> and Paolo Carloni<sup>\*,†</sup>

Contribution from the International School for Advanced Studies (ISAS/SISSA) and INFN-Democritos Modeling Center for Research in Atomistic Simulation, via Beirut 4, 34014 Trieste, Italy, and Nanochemistry Research Institute, Curtin University of Technology, P.O. Box U1987, Perth 6845, Western Australia

Received November 16, 2005; E-mail: carloni@sissa.it

**Abstract:** Recent measurements of trans-hydrogen bond deuterium isotope effects (DIEs) on  $^{13}\text{C}$  chemical shifts in nucleic acids (Vakonakis, I.; LiWang, A. C. *J. Biomol. NMR* **2004**, *29*, 65; *J. Am. Chem. Soc.* **2004**, *126*, 5688) have led to intriguing results: (i) the DIEs of A:T pairs in DNA are about 5 ppb smaller than those of A:U in RNA and (ii) A:T DIEs vary by as much as 13 ppb among the oligonucleotides. The first observation suggests that inter-base H-bonds in RNA may be stronger than those in DNA, while the second indicates that the conformation of the base pair modulates the transmission of the isotope effect across the hydrogen bond. In an effort at providing a rationale — so far unknown — for the observed DIEs in nucleic acids, density functional theory and hybrid Car–Parrinello/molecular mechanical calculations of DIEs on nucleosides and nucleotides in the gas phase and in aqueous solution have been performed. The calculations suggest that (i) the DIE in an isolated A:T base pair differs from that in an A:U base pair because of the changes in the magnetic properties caused by the replacement of a methyl group on passing from U to T, (ii) the DIEs depend crucially on the conformation of the base pairs, and (iii) the DIEs are strongly affected by magnetic and electrostatic interactions with the surrounding environment.

### Introduction

Deuterium isotope effects (DIEs) on  $^{13}\text{C}$  chemical shifts provide very valuable information on the nature of H-bonding interactions.<sup>1–4</sup> They can be easily detected: if the H atom involved in the H-bond is the site of isotopic substitution, the DIE can be as large as 1 ppm. Recently, DIE measurements provided important information on base-pair H-bonding in nucleic acids.<sup>5,6</sup> First, it was shown that, in five DNA duplexes, DIEs for A:T pairs are generally smaller than the corresponding DIEs for A:U in the RNA homologues.<sup>5</sup> Although this could be taken as an indication of stronger H-bonding in the A:U@RNA relative to A:T@DNA,<sup>5</sup> quantum chemical calculations at the density functional theory (DFT) level pointed to an absence of correlation between H-bond strength and the chemical shifts<sup>7</sup> and, along with calculations at the ab initio correlated level, to a similarity in the energy of formation of A:T@DNA and A:U@RNA base pairs.<sup>8</sup> Thus, factors other than H-bond strength must play a crucial role in the observed differences.

Second, A:T@DNA DIEs vary by as much as 13 ppb among the oligonucleotides,<sup>6</sup> indicating that the local conformation of the DNA duplex influences the transmission of the isotope effect across the hydrogen bonds. However, the key factors for this modulation are still to be understood.

First-principle calculations of NMR chemical shifts in biological systems have been shown to help rationalize experimental data.<sup>9</sup> Here, on the basis of DFT and quantum mechanical (QM)/molecular mechanical (MM) calculations, it is shown that there is an intrinsic DIE difference between A:T and A:U, caused by the difference in electronic structure of the two base pairs due to the replacement of a methyl group with a hydrogen atom. In addition, the base-pair conformation largely affects the DIE, supporting a previous hypothesis.<sup>6</sup> In particular, shear, stretch, and opening, the parameters defining the geometry of the H-bond, play a major role. Finally, these calculations provide evidence that electrostatic and magnetic interactions between the base pair and the surrounding environment can have a large influence on the DIE.

### Methods

**Quantum Chemical Methods.** DFT calculations were performed on the A:T and A:U base pairs in vacuo. Calculations were also carried out for A:T embedded in DNA duplexes in aqueous solution, using a hybrid DFT/MM approach. The structural features turn out to be similar

<sup>†</sup> ISAS/SISSA and INFN-DEMOCRITOS.

<sup>‡</sup> Curtin University of Technology.

<sup>§</sup> Current address: Parc Científic de Barcelona, C/ Josep Samitier 1-5, 08028 Barcelona, Spain.

- (1) Reuben, J. *J. Am. Chem. Soc.* **1987**, *109*, 316–321.
- (2) Smirnov, S. N.; Golubev, N. S.; Denisov, G. S.; Benedict, H.; Schah-Mohammadi, P.; Limbach, H. H. *J. Am. Chem. Soc.* **1996**, *118*, 4094–4101.
- (3) Perrin, C. L.; Nielson, J. B. *J. Am. Chem. Soc.* **1997**, *119*, 12734–12741.
- (4) Abildgaard, J.; Bolvig, S.; Hansen, P. E. *J. Am. Chem. Soc.* **1998**, *120*, 9063–9069.
- (5) Vakonakis, I.; LiWang, A. C. *J. Am. Chem. Soc.* **2004**, *126*, 5688–5689.
- (6) Vakonakis, I.; LiWang, A. C. *J. Biomol. NMR* **2004**, *29*, 65–72.
- (7) Swart, M.; Guerra, C. F.; Bickelhaupt, F. M. *J. Am. Chem. Soc.* **2004**, *126*, 16718–16719.
- (8) Perez, A.; Sponer, J.; Jurecka, P.; Hobza, P.; Luque, F. J.; Orozco, M. *Chem.–Eur. J.* **2005**, *11*, 5062–5066.
- (9) Piana, S.; Sebastiani, D.; Carloni, P.; Parrinello, M. *J. Am. Chem. Soc.* **2001**, *123*, 8730–8737.

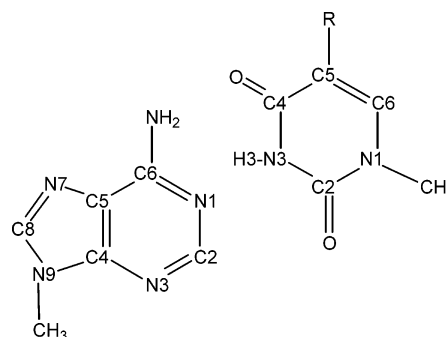
(data not shown) to those of previous calculations at the DFT<sup>10–12</sup> and ab initio levels.<sup>13,14</sup>

The quantum problem was solved within the DFT framework.<sup>15,16</sup> Valence orbitals were expanded with a plane wave basis set up to 70 Ry. Martins–Troullier pseudopotentials<sup>17</sup> were used to describe the core electron–valence shell electron interactions. The BLYP exchange–correlation functional was used.<sup>18</sup> This functional has already been used to predict NMR quantities in a variety of chemical<sup>19</sup> and biochemical<sup>19</sup> studies. Geometry optimizations were achieved with the GDIIS method,<sup>20</sup> setting a convergence criterion of  $5 \times 10^{-4}$  for the largest component of the atomic forces.

QM/MM calculations were performed within a fully Hamiltonian coupling scheme between the DFT region (a single A:T pair) and the classical regions (the rest of selected oligonucleotides (see below) in aqueous solution, in the presence of counterions).<sup>21</sup> The interface between the QM and MM subsystems was located at the C1'–N9@A and C1'–N1@T bonds. Dangling bonds were saturated by hydrogen atoms. Spurious electrostatic interactions between the capping hydrogens and close-by classical atoms were excluded from the QM/MM Hamiltonian according to ref 22. Electrostatic interactions were taken into account within a multilayer approach.<sup>21,22</sup> The QM/MM electrostatic interactions were evaluated as follows: (i) a modified Coulomb interaction between the QM electronic density and the MM atoms within 5.3 Å of any QM atom; (ii) Coulomb interactions between D-RESP point charges<sup>23</sup> centered on the QM atoms and RESP charges<sup>24</sup> on the MM atoms between 5.3 and 15.9 Å from any QM atom; and (iii) electrostatic interactions between the MM atoms and a multipole expansion representing the charge distribution of the QM region<sup>21</sup> beyond 15.9 Å. Bonded and van der Waals interactions between the QM and MM parts were accounted for by the AMBER force field.<sup>25</sup> The DFT calculations were performed with the CPMD code,<sup>26</sup> while a modified version of the GROMOS96<sup>27</sup> code was used for the MM region in QM/MM calculations.

**Calculation of NMR Properties.** In this work, it is assumed that the potential energy surface (PES) of the base pairs required for the calculation of DIEs can be reduced to the N3@T–H3@T and N3@U–H3@U stretching for A:T and A:U, respectively (see Chart 1). This assumption is based on two facts: (i) Hartree–Fock calculations on small molecules have shown that DIEs are dominated by bond stretching,<sup>28</sup> and (ii) a normal-mode analysis performed here on the Watson–Crick A:T pair (the geometry of the pair is optimized at the BLYP level of theory<sup>18</sup>) predicts that the mode involving the N3–

**Chart 1.** A:T and A:U Watson–Crick Base Pairs<sup>a</sup>



<sup>a</sup> R = CH<sub>3</sub> in A:T, R = H in A:U.

H3@T bond is basically decoupled from the motion of the rest of the system. Indeed, this mode has a 98% projection on the N3–H3@T distance; in addition, the frequency of this mode changes by as much as 25% upon isotopic substitution.

The PES can be then calculated by fixing the N3–H3 distance (Chart 1) at increasing values (by 0.1 Å) and by either relaxing the other degrees of freedom (relaxed scan) or keeping them fixed (rigid scan). Most of the DIE calculations were performed within the rigid scan approach, which provides a qualitative picture of the dependence of the DIE on base-pair conformation while reducing the cost of the calculation. However, both approaches were used for the comparison of DIEs between A:U and A:T, for which a semiquantitative estimate is deemed necessary.

Shielding constants were calculated through the variational approach of density functional perturbation developed by Sebastiani et al.<sup>29</sup> for each point along the PES. The calculated energy and shielding values (20 points) were fitted to a polynomial of eighth degree and of sixth degree, respectively, which provided a good fit. The 1D nuclear Schrödinger equation for the proton (reduced mass of 1 au) and the deuterium (reduced mass 2 au) was then solved variationally using the calculated PES. Harmonic oscillator basis set functions were used to describe the vibrational ground-state wave function as in ref 30. One hundred terms turned out to ensure that the calculated DIEs were converged. The DIEs were calculated as the difference between the shielding expectation values over the proton and deuterium probability distributions:<sup>28</sup>

$$\text{DIE} = \langle \Psi_{\text{H}} | \sigma | \Psi_{\text{H}} \rangle - \langle \Psi_{\text{D}} | \sigma | \Psi_{\text{D}} \rangle \quad (1)$$

DIE calculations of A:T and A:U in vacuo were carried out for the following conformations: (i) the optimized A:T and A:U structures; (ii) 13 different geometries of the A:T pair obtained by combining the optimized geometries of A and T, using the program X3DNA<sup>31</sup> (in these conformations, only one base-pair parameter at a time was varied); and (iii) 23 conformations of the A:T pair built with base-pair parameters from MD simulations of base pair 5 of the d(C-GAAAATTTTCG)<sub>2</sub> oligonucleotide in aqueous solution (see Supporting Information).

QM/MM DIE calculations were performed for the following base pairs embedded in the duplex environment (see Supporting Information): Bp5@d1, Bp4@d2, Bp8@d2, Bp3@d3, and Bp6@d3. For each base pair, a snapshot extracted from MD simulations underwent 500 QM/MM NVE-MD steps, followed by 1000 steps of QM/MM annealing (with scaling factor of 0.99). The final conformation was used for the calculation of the DIE. Comparison was made with calculations in vacuo of the DIEs of the base pairs only and of the

- (10) Popelier, P. L. A.; Joubert, L. *J. Am. Chem. Soc.* **2002**, *124*, 8725–8729.
- (11) Carloni, P.; Andreoni, W. *J. Phys. Chem.* **1996**, *100*, 17797–17800.
- (12) Guerra, C. F.; Bickelhaupt, F. M.; Snijders, J. G.; Baerends, E. J. *J. Am. Chem. Soc.* **2000**, *122*, 4117–4128.
- (13) Hobza, P.; Sponer, J.; Cubero, E.; Orozco, M.; Luque, F. J. *J. Phys. Chem. B* **2000**, *104*, 6286–6292.
- (14) Sponer, J.; Hobza, P. *J. Phys. Chem. A* **2000**, *104*, 4592–4597.
- (15) Hohenberg, P.; Kohn, W. *Phys. Rev. B* **1964**, *136*, 864–871.
- (16) Kohn, W.; Sham, L. J. *Phys. Rev. A* **1965**, *140*, 1133–1138.
- (17) Troullier, N.; Martins, J. L. *Phys. Rev. B* **1991**, *43*, 1993–2006.
- (18) Lee, C.; Yang, W.; Parr, R. G. *Phys. Rev. B* **1988**, *37*, 785–789. Becke, A. D. *Phys. Rev. A* **1988**, *38*, 3098–3100.
- (19) Sebastiani, D.; Parrinello, M. *Chemphyschem* **2002**, *3*, 675–679.
- (20) Csaszar, P.; Pulay, P. *J. Mol. Struct.* **1984**, *114*, 31–34.
- (21) Laio, A.; VandeVondele, J.; Roethlisberger, U. *J. Chem. Phys.* **2002**, *116*, 6941.
- (22) Laio, A.; Gervasio, F. L.; VandeVondele, J.; Sulpizi, M.; Rothlisberger, U. *J. Phys. Chem. B* **2004**, *108*, 7963–7968.
- (23) Laio, A.; VandeVondele, J.; Roethlisberger, U. *J. Phys. Chem. B* **2002**, *106*, 7300–7307.
- (24) Wang, J. M.; Cieplak, P.; Kollman, P. A. *J. Comput. Chem.* **2000**, *21*, 1049–1074.
- (25) Cornell, W. D.; Cieplak, P.; Bayly, C. I.; Gould, I. R.; Merz, K. M., Jr.; Ferguson, D. M.; Spellmeyer, D. C.; Fox, T.; Caldwell, J. W.; Kollman, P. A. *J. Am. Chem. Soc.* **1995**, *117*, 5179–5197.
- (26) Hutter, J.; Alavi, A.; Deusch, T.; Silvestri, W.; Parrinello, M. *CPMD; MPI fuer Festkoerperforschung Stuttgart and IBM Zurich Research Laboratory*, 2000.
- (27) van Gunsteren, W. F. *Biomolecular Simulation: The GROMOS96 Manual and User Guide*; Hochschulverlag AG der ETH Zuerich: Zuerich/Groningen, 1996.
- (28) Jameson, C. J. *Annu. Rev. Phys. Chem.* **1996**, *47*, 135–169.

- (29) Sebastiani, D.; Parrinello, M. *J. Phys. Chem. A* **2001**, *105*, 1951–1958.
- (30) Wilson, E. B.; Decius, J. C.; Cross, P. C. *Molecular vibrations: the theory of infrared and Raman vibrational spectra*; McGraw-Hill: New York, 1955.
- (31) Lu, X. J.; Olson, W. K. *Nucleic Acids Res.* **2003**, *31*, 5108–5121.

**Table 1.** Calculated NMR Properties of A:T and A:U in the Ideal, Planar Watson–Crick Base-Pair Conformation for *Rigid* and *Relaxed* Scans

base	DIE at A (ppb)					DIE at U/T (ppb)				$\Delta r^c$ (Å)	$\partial\sigma(\text{C2@A})/\partial r$ (ppm/Å)
	atom C2	atom C4	atom C5	atom C6	atom C8	atom C2	atom C4	atom C5	atom C6		
A:T <sup>a</sup>	78.3	−15.6	−11.4	49.6	−42.3	−38.2	−73.6	8.7	46.4	0.021	4.8
A:U <sup>a</sup>	79.6	−16.1	−11.3	50.3	−42.9	−33.6	−83.5	3.3	48.7	0.021	4.9
A:T <sup>b</sup>	128.5	−56.0	−75.2	−28.5	−64.2	−196.4	−262.9	−27.5	24.1	0.021	15.3
A:U <sup>b</sup>	146.5	−56.5	−77.8	−23.8	−65.6	−195.8	−301.6	−42.9	17.2	0.021	17.1

<sup>a</sup> 1D *rigid* PES and shielding surface. <sup>b</sup> 1D *relaxed* PES and shielding surface. <sup>c</sup>  $\Delta r = \langle r \rangle_{\text{H}} - \langle r \rangle_{\text{D}}$ .

base pair surrounded by its adjacent nucleobases, not including sugars and phosphate backbone in the models, treated at the DFT-BLYP level of theory.

Electronic density difference calculations between the A:T and A:U base pairs were performed for the optimized A:T pair and a model of the A:U base pair at the optimized A:T geometry, replacing the methyl group at C5@T with a hydrogen atom and optimizing its position. The isotropic shielding density distributions of atom C2@A,  $\sigma^{\text{C2@A}}(\mathbf{r})$ , were calculated for the same nucleobase conformations, following the equations

$$\sigma^{\text{C2@A}}(\mathbf{r}) = \frac{\sigma_{xx}^{\text{C2@A}}(\mathbf{r}) + \sigma_{yy}^{\text{C2@A}}(\mathbf{r}) + \sigma_{zz}^{\text{C2@A}}(\mathbf{r})}{3}$$

$$\sigma_{\alpha\beta}^{\text{C2@A}} = -\frac{1}{cB} \int d\mathbf{r} \left[ \frac{\mathbf{r} - \mathbf{r}_{\text{C2@A}}}{|\mathbf{r} - \mathbf{r}_{\text{C2@A}}|^3} \times \mathbf{J}_{\beta}(\mathbf{r}) \right]_{\alpha}$$

$$= \int d\mathbf{r} \sigma_{\alpha\beta}^{\text{C2@A}}(\mathbf{r})$$

where the second equation defines the shielding density<sup>32,33</sup> and  $c$  is the speed of light,  $\mathbf{r}_{\text{C2@A}}$  the position vector of atom C2@A, and  $\mathbf{J}_{\beta}(\mathbf{r})$  the current density induced by a magnetic field  $\mathbf{B}$  in the  $\beta$  direction.

## Results and Discussion

Here, DFT and molecular dynamics simulations were used to investigate, at the qualitative level, (i) why observed trans-hydrogen bond DIEs on <sup>13</sup>C shieldings are (generally) larger in RNA than in DNA and (ii) the dependence of the DIEs on the base-pair conformation.

**Differences between DIEs in DNA and in RNA.** The observed differences in DIEs may result from the different conformation of the DNA and RNA duplexes and/or from an intrinsic difference between the two base pairs. To assess the relative importance of these two contributions, (i) the intrinsic DIEs in the two base pairs and (ii) the distributions of conformational parameters of the A:T and A:U pairs embedded in DNA and RNA duplexes were compared.

The calculated DIEs in A:T and A:U pairs turn out to differ mostly for pyrimidine atoms, where larger differences are observed for atoms closer to the site of substitution (C5 in pyrimidines, Table 1). The difference between the calculated DIEs at C2@A is  $\sim 1$  ppb within the rigid PES scan, while it is 18 ppb within the relaxed scan. This can be compared with the experimental average difference of DIEs at C2@A between DNA and RNA duplexes of about 5 ppb.<sup>5</sup> The DIE on C2@A and that on C4@T are of opposite signs, as experimentally observed.<sup>6</sup>

It is reported in the literature that DIEs calculated with this approach generally correlate well with experimental DIEs,<sup>4</sup>

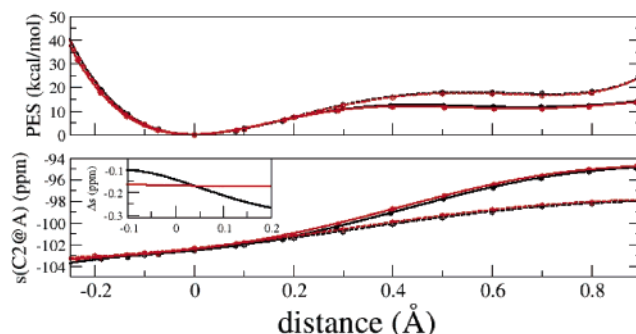


**Figure 1.** DFT calculations on A:T and A:U base pairs: 1D potential energy surface (PES, top) and shielding surface for C2@A ( $s(\text{C2@A})$ , bottom) for the A:T (black circles and lines) and A:U (red circles and lines) base pairs, within the *relaxed* (solid circles and continuous lines) and the *rigid* (open circles and dotted lines) scan approaches (see text). Circles are the calculated values, while lines are the best polynomial fit to the data (see text). Inset: Difference between the A:T and A:U shielding surfaces for C2@A ( $\Delta s(\text{C2@A})$ ) within the relaxed (black line) and rigid (red line) scan approaches. H-bond parameters for the optimized structures are the same for A:T and A:U:  $d(\text{N1@A}, \text{N3@T/U}) = 2.91$  Å,  $d(\text{N1@A}, \text{H3@T/U}) = 1.86$  Å,  $d(\text{N3@T/U}, \text{H3@T/U}) = 1.05$  Å,  $\angle(\text{N1@A}, \text{H3@T/U}, \text{N3@T/U}) = 179.8^\circ$ .

although a quantitative agreement is in general not achieved.<sup>34</sup> It is therefore concluded that, while there is an intrinsic difference of a few ppb between the DIEs at C2@A in A:T and C2@A in A:U, a more precise estimate of this difference is not possible.

The calculated difference of the DIEs at C2@A between A:T and A:U may result either from a different PES or from different shielding surfaces. The relative importance of these two contributions can be assessed assuming that the following approximation to eq 1, based on a Taylor expansion,<sup>4</sup> holds:

$$\text{DIE} = (\partial\sigma(\text{C})/\partial r) (\langle r \rangle_{\text{H}} - \langle r \rangle_{\text{D}}) \quad (2)$$

$\partial\sigma(\text{C})/\partial r$  is the derivative of the shielding of atom C at the PES minimum, which depends on the shielding surface.  $\langle r \rangle_{\text{H}}$  and  $\langle r \rangle_{\text{D}}$  are the average N3–H3@T/U distances over the proton and deuterium probability distributions, respectively:  $\langle r \rangle_{\text{H/D}} = \langle \Psi_{\text{H/D}} | r | \Psi_{\text{H/D}} \rangle$ . Their difference reflects differences in the PES curvature. It turns out that  $(\langle r \rangle_{\text{H}} - \langle r \rangle_{\text{D}})$  is the same in A:U and A:T (Table 1), and indeed at the minimum the two PESs are nearly identical, both within the rigid and within the relaxed PES scans (Figure 1). In contrast,  $\partial\sigma(\text{C})/\partial r$  differs in the two systems (Table 1), indicating that the difference in DIEs between A:T and A:U results mainly from the magnetic properties of thymine relative to uracil.

The difference in the electronic and magnetic shielding densities between A:T and A:U was calculated. The electronic

(32) Jameson, C. J.; Buckingham, A. D. *J. Chem. Phys.* **1980**, *73*, 5684.

(33) Keith, T. A.; Bader, R. F. W. *Chem. Phys. Lett.* **1992**, *194*, 1–8.

(34) Stare, J.; Jezierska, A.; Ambrozic, G.; Kosir, I. J.; Kidric, J.; Koll, A.; Mavri, J.; Hadzi, D. *J. Am. Chem. Soc.* **2004**, *126*, 4437–4443.



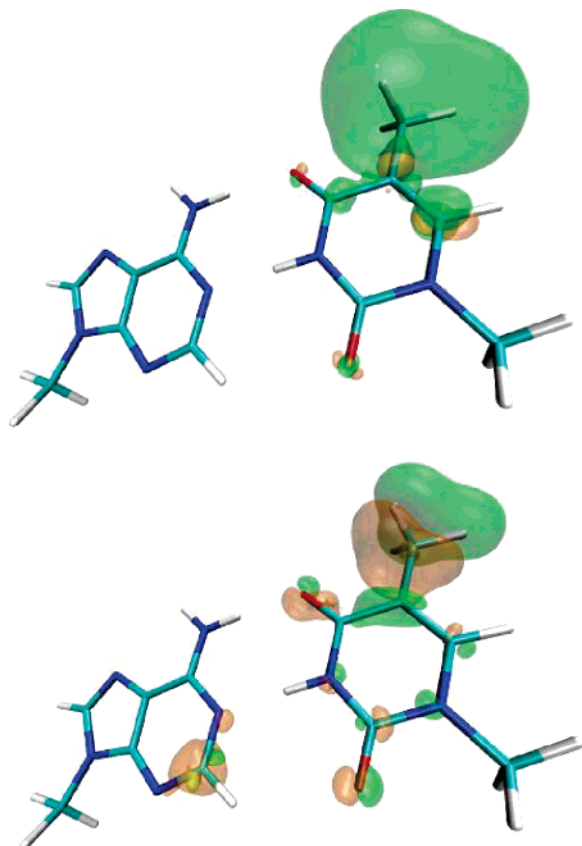


**Figure 2.** (Top) Electronic density difference between A:T and A:U base pairs. The isodensity surfaces at 0.001 and  $-0.001 \text{ e } \text{\AA}^{-3}$  are plotted in green and orange, respectively. (Bottom) Shielding density difference between A:T and A:U base pairs. The isoshielding density surfaces at 0.001 and  $-0.001 \text{ ppm } \text{\AA}^{-3}$  are plotted in green and orange, respectively. The structure of the A:T base pair is superimposed on the isosurfaces.

density difference between the two base pairs shows an increase of the charge density on the T ring with respect to U, as expected due to the electron-donating character of the methyl group (Figure 2). The charge density difference is mostly localized on the thymine/uracil atoms close to the site of substitution (C4@T/U and C6@T/U), while only minor changes are observed at N3@T/U and on the A heterocycle. In contrast, the shielding density displays substantial differences along the H-bond and on C2@A (Figure 2). Consistent with these findings, the calculated association energy of A:T is only marginally smaller (by 0.05 kcal/mol) than that of A:U in their optimized conformations at the DFT-BLYP level. This result is also in line with previous calculations at the DFT and ab initio correlated levels<sup>7,8</sup> of these two base pairs in a variety of conformations. In summary, no indication of a greater intrinsic stability of A:U pairs with respect to A:T pairs is found in these calculations. On the other hand, it is demonstrated that the methyl group substitution in thymine can lead to a significant perturbation of the magnetic properties of adenine and therefore affect the DIE.

The dependence of DIEs on the conformational properties of the base pairs was investigated by performing multinano-second classical MD simulations of several DNA and RNA duplexes. The accuracy of these calculations was assessed by comparison with the available experimental data (see Supporting Information). It would be best to compare experimental DIEs with experimental structures of RNA and DNA. Unfortunately,

**Table 2.** MD-Averaged A:T and A:U Base-Pair Parameters<sup>a</sup>

base-pair parameter	A:T	A:U
shear ( $\text{\AA}$ )	0.11 (0.02)	0.07 (0.02)
stretch ( $\text{\AA}$ )	$-0.086$ (0.005)	$-0.056$ (0.011)
stagger ( $\text{\AA}$ )	0.003 (0.078)	$-0.169$ (0.106)
buckle (deg)	6.1 (3.7)	$-3.5$ (3.7)
propeller (deg)	$-15.2$ (3.3)	$-14.1$ (1.9)
opening (deg)	0.25 (0.65)	0.67 (0.91)

<sup>a</sup> Standard error is given in parentheses.

to the best of our knowledge, experimental data are available only for one of the structures considered here (**d1**). Thus, it is necessary to resort to theoretical models obtained from MD simulations in order to compare conformational properties of the duplexes in solution. The average and distribution of the shear, stretch, stagger, buckle, propeller, and opening base-pair parameters were examined. These parameters describe the local geometry of the base pair and have been proposed to play a key role for the DIEs.<sup>5,6</sup>

The MD-averaged values obtained from the simulations are rather similar (Table 2), and their distributions are completely overlapping for shear and opening and largely overlapping for stretch, stagger, buckle, and propeller (Figure 3a). Stretch and propeller are generally less negative for A:U pairs, while stagger and buckle are generally shifted toward negative values in A:U pairs with respect to A:T. Buckle is the most variable parameter. Although it is expected that the DIEs should depend somewhat on the base-pair conformation, scatter plots of the calculated base-pair parameters with respect to the experimental DIEs do not reveal any appreciable degree of correlation (Figure 3b), suggesting either that a combination of several parameters may contribute to the magnitude of the DIE or that other effects are important in determining the observed DIE.

It is concluded that there is an intrinsic difference between DIEs in A:T and A:U base pairs that should be attributed to the different magnetic properties of the T and U nucleobases. A simple analysis of base-pair conformations does not show any correlation with the experimental base pairs, indicating either that the relationship is more complex or that other factors are important for the modulation of the DIE.

**DIEs in Different A:T Conformations.** The dependence of the DIE with respect to base-pair conformation was further investigated. To this aim, base-pair parameters were varied one at a time from the ideal, planar Watson–Crick base-pair conformation and the DIE for each conformation was calculated. The results of these calculations are presented in Figure 4 and suggest the following: (i) The parameters that most influence the H-bond geometry (shear, stretch, and opening) are also the parameters that have the largest effects on the DIEs (Figure 4a); stagger also has a significant contribution, while buckle and propeller have less pronounced effects (Figure 4a). (ii) For shear and opening, the trend depends on the atom where the DIE is calculated: higher shear and opening correspond to smaller DIE at C2@A, while the opposite trend is displayed by the DIE at C4@T (Figure 4a). These opposing trends explain the weak correlation between DIEs at C4@T and C2@A observed in the NMR experiments.<sup>5</sup>

Consistent with previous conclusions,<sup>7</sup> scatter plots of the DIEs at C2@A and C4@T with respect to the base-pair binding energy indicate that a large DIE does not necessarily correspond to a stronger interaction (Figure 4b). (As no attempt is made

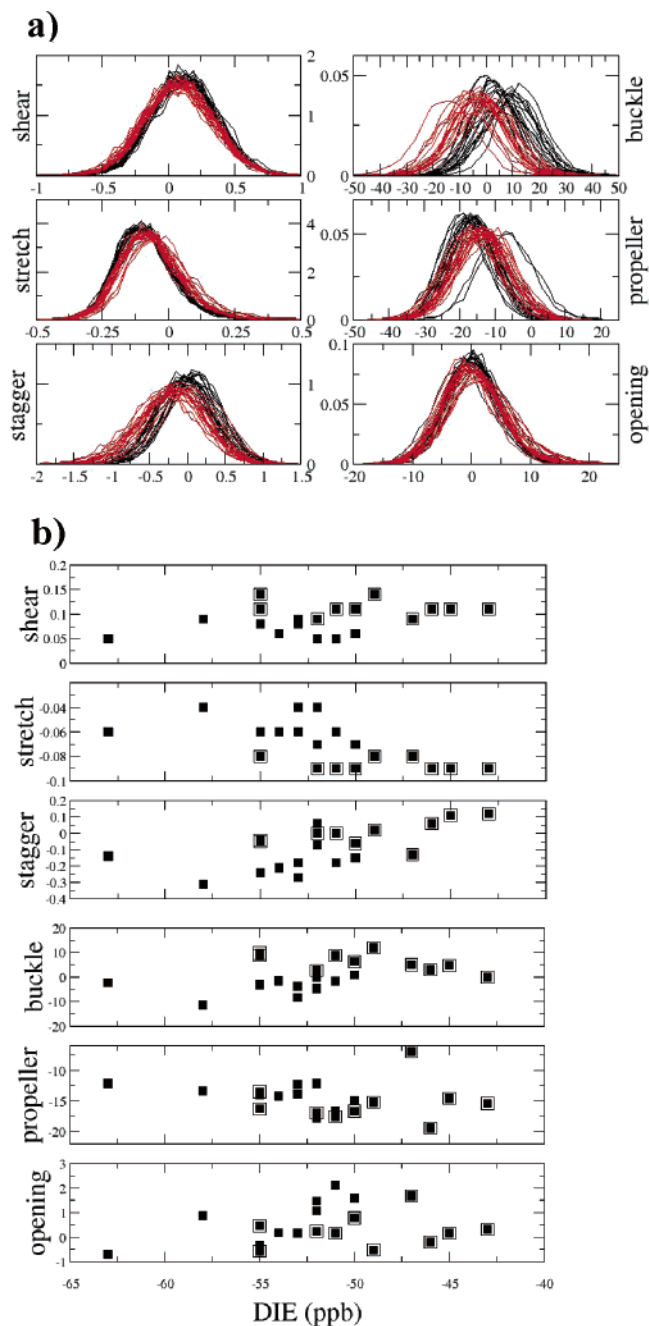


**Figure 3.** Classical MD simulations of the following oligonucleotides:  $d(\text{CGCGAATTCGCG})_2$ ,  $r(\text{CGCGAAUUCGCG})_2$ ,  $d(\text{GTTTTAAAACG})_2$ ,  $r(\text{CGUUUUAAAACG})_2$ ,  $d(\text{CGAAAATTTTCG})_2$ , and  $r(\text{CGAAAAUUUUCG})_2$ <sup>5,6</sup> (for details of the MD simulations, see Supporting Information). (a) Distributions of base-pair parameters for A:T (black lines) and A:U (red lines) pairs in the duplexes investigated. Notice that buckle is the only parameter for which the distribution is not completely symmetric. (b) Scatter plot of MD-averaged base-pair parameters and experimental DIEs.<sup>5,6</sup> Black frames highlight values for A:T pairs. Parameters for sequence-related base pairs were averaged.

here at partitioning the energy, it is not possible to investigate the dependence of the DIE only on the strength of the  $\text{N1@A} \cdots \text{H3@T} - \text{N3@T}$  H-bond.) Indicators of the strength of H-bonds, such as shielding of hydrogens involved in H-bonds<sup>1,35,36</sup> (here  $\text{H3@T}$ ) and distances between donor and acceptor atoms<sup>37</sup>

(35) Cleland, W. W. *Arch. Biochem. Biophys.* **2000**, *382*, 1–5.

(36) Del Bene, J. E.; Perera, S. A.; Bartlett, R. J. *J. Phys. Chem. A* **1999**, *103*, 8121–8124.

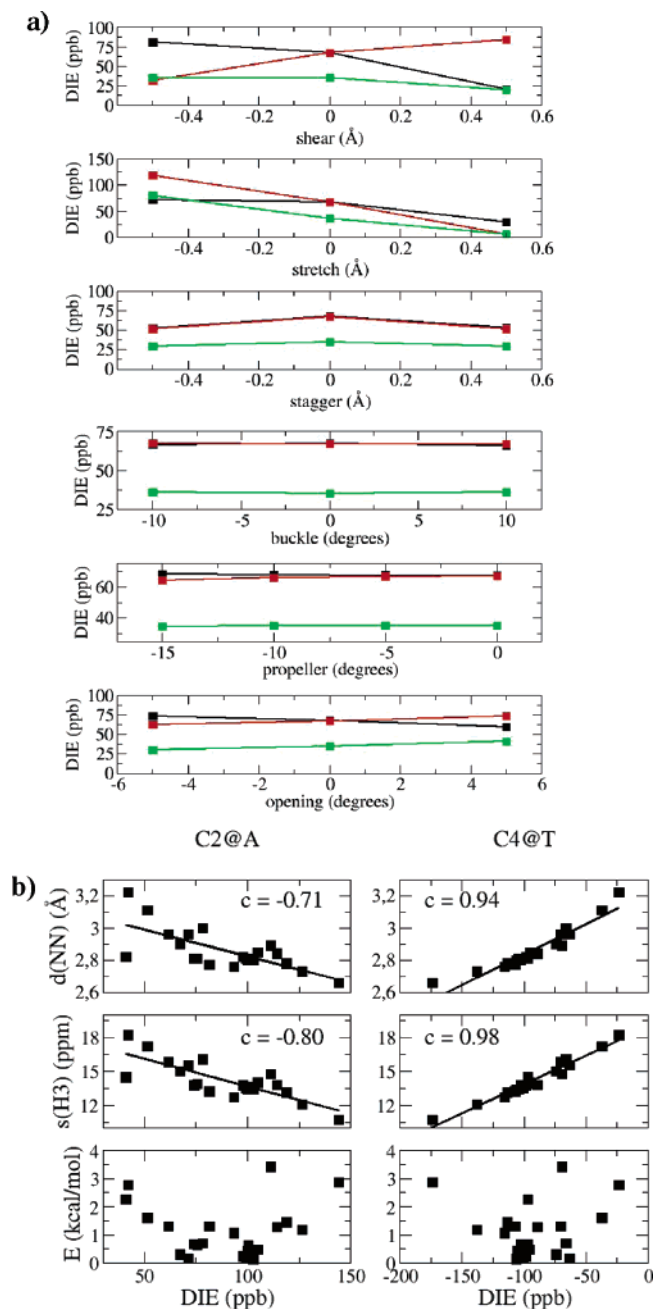


**Figure 4.** DFT calculations of A:T base pair. (a) Profile of C2@A (black line), C4@T (red line), and C2@T (green line) DIEs with variations of one base-pair parameter. (b) Scatter plots of the distance between N1@A and N3@T ( $d(\text{NN})$ , top), the shielding at H3 ( $s(\text{H3})$ , middle), and base-pair energy ( $E$ , bottom) with respect to the DIEs at C2@A (left) and C4@T (right). Black lines are the least-squares fits to the data.

(here  $d(\text{N1@A} - \text{N3@T})$ , correlate well with the DIE on C4@T (correlation coefficients 0.98 and 0.94, Figure 4b), while the correlation is weaker with DIE on C2@A (correlation coefficients  $-0.80$  and  $-0.71$ , respectively). These results are completely consistent with a recent NMR study on DNA and RNA dodecamers.<sup>38</sup> This study points to a correlation of the DIE on C2@A and  $J_{\text{NH}}$ , the one-bond  $^{15}\text{N} - ^1\text{H}$  coupling constant, the latter being an indicator of the H-bond length.<sup>38</sup>

(37) Harris, T. K.; Mildvan, A. S. *Proteins: Struct., Funct. Genet.* **1999**, *35*, 275–282.

(38) Manalo, M. N.; Kong, X.; LiWang, A. *J. Am. Chem. Soc.* **2005**, *127*, 17974–17975.

**Table 3.** DIEs (ppb) Calculated for Selected Base Pairs in Different DNA Duplexes for a Conformation from MD Simulation within Different Approaches

base	A					T			
	C2	C4	C5	C6	C8	C2	C4	C5	C6
atom									
single bp	57.6	−19.6	−12.6	57.5	−43.9	−39.4	−72.7	18.9	42.8
QM/MM	46.7	−19.6	−16.9	52.3	−44.1	−36.1	−73.7	19.7	41.1
triplet	74.3 (29%)	−26.3	−10.9	66.8	−48.8	−42.5	−85.1 (17%)	16.4	44.7
single bp	81.9	−20.1	−17.0	65.6	−48.4	−46.4	−93.6	22.0	50.3
QM/MM	68.0	−17.4	−21.2	61.7	−46.1	−40.1	−96.4	23.9	46.0
triplet	93.5 (14%)	−22.1	−12.7	64.5	−48.5	−45.7	−96.3 (3%)	18.1	48.4
single bp	52.4	−9.8	−16.4	31.1	−28.8	−21.4	−44.1	11.7	30.6
QM/MM	41.5	−10.4	−16.3	25.4	−26.3	−16.0	−41.7	13.6	28.4
triplet	57.4 (10%)	−11.2	−20.7	36.1	−29.9	−23.3	−44.3 (0%)	10.2	29.7
single bp	84.0	−19.7	−16.5	51.1	−42.9	−42.8	−74.6	14.0	47.2
QM/MM	90.8	−21.7	−21.7	53.7	−48.0	−46.4	−88.8	18.0	53.4
triplet	111.9 (33%)	−26.6	−18.3	70.6	−50.4	−49.5	−89.4 (20%)	18.2	55.5
single bp	97.9	−16.6	−18.2	50.7	−45.8	−46.0	−77.4	13.9	49.6
QM/MM	112.4	−21.5	−27.7	65.0	−57.7	−56.2	−108.6	22.7	62.7
triplet	120.1 (23%)	−23.0	−19.3	64.1	−54.4	−55.8	−91.1 (18%)	14.7	53.1

Indeed, the degree of correlation between  $J_{NH}$  and the DIE found by Manalo and co-workers is similar to the correlation found in our calculations between H-bond length and DIE (Figure 4b). As a given  $d(N1@A-N3@T)$  distance may result from different base-pair parameters, the lower level of correlation between  $d(N1@A-N3@T)$  and the DIE on C2@A compared to the DIE on C4@T is the result of the opposing trends displayed by the DIE at these two atoms with respect to the shear and opening parameters.

So far, only isolated base pairs were considered. To investigate the effects of the environment, the DIEs were compared with values calculated within a QM/MM approach where the A:T base pair is treated at the DFT level, while the rest is described with the AMBER force field.<sup>25</sup> The QM/MM DIEs

differ from those calculated in vacuo by  $-14$  to  $+16$  ppb (Table 3). These contributions, which clearly are related to the electrostatic field, are comparable to the effects of the conformation. However, due to the limited number of conformations used, any attempt to relate this contribution to a simple descriptor of the electrostatic field has not been successful.

Note that the opposing changes in the DIEs calculated for Bp3@d3 and Bp5@d1 when single base pair and QM/MM results are compared is probably due to the fact that a  $Na^+$  ion coordinates Bp3@d3, while no counterions are close to Bp5@d1 in the conformation used in the calculation. This points to the relevance of counterions for electronic properties, in agreement also with ref 39.

Finally, DFT calculations on the base pair of interest, surrounded by its adjacent nucleobases treated at the QM level of theory, were performed. These calculations allow us to estimate the shielding contributions arising from the stacked bases, which cannot be captured by the QM/MM calculations (Table 3). The conformations of the surrounding base pairs were taken from the corresponding QM/MM calculation. The resulting DIEs increase by 10–30% relative to those of the isolated A:T pairs (Table 3). This effect appears to be modulated by the overlap between contiguous base pairs: a larger overlap corresponding to a smaller shift with respect to the isolated base pair (Figure 5).

## Conclusions

The effects of electronic structure, base-pair conformation, and duplex environment on the DIE have been investigated by performing DFT calculations of DIEs in A:T and A:U base pairs. These calculations show that DIEs are strongly influenced by the duplex conformation. Several factors are important in this respect: (i) the base-pair conformation, (ii)

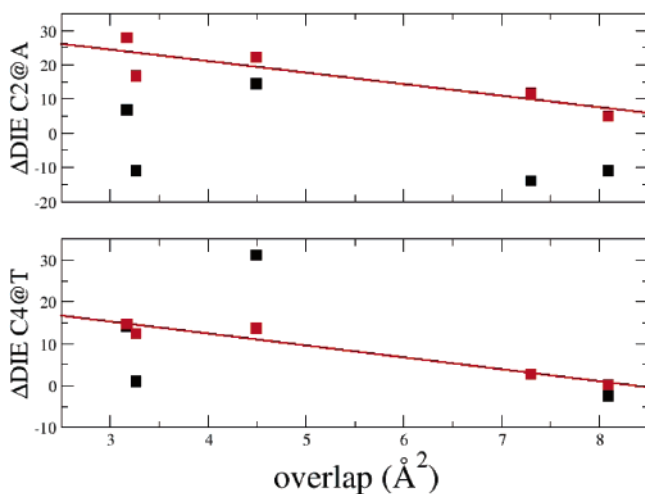


**Figure 5.** Difference ( $\Delta$ ) between the DIEs calculated within the QM/MM approach (black squares) and between DFT calculations of a triplet of base pairs (red squares) and the isolated base-pair calculations. Differences are plotted as a function of the overlap between the central and the adjacent base pairs.<sup>31</sup> The red lines are the best linear fits to the red squares (correlation coefficients are  $-0.96$  and  $-0.97$  for  $\Delta$ DIE C2@A and  $\Delta$ DIE C4@T, respectively).

(39) Barnett, R. N.; Cleveland, C. L.; Joy, A.; Landman, U.; Schuster, G. B. *Science* **2001**, *294*, 567–571.

the electric field generated by the duplex and the counterions, and (iii) to a lesser extent, the magnetic field generated by the adjacent base pairs. None of these three contributions is clearly dominant over the other two. These findings highlight the difficulty of directly relating calculated DIEs to a single structural parameter, like an H-bond distance. Finally, our calculations suggest that the observed difference of DIEs in DNA and RNA duplexes may be caused, at least in part, to the different electronic properties of the A:T and A:U base pairs, although significant contributions of the biomolecular frame cannot be excluded.

**Acknowledgment.** The authors acknowledge INFM and MURST for financial support and CINECA for computational resources. S.P. acknowledges the Australian Research Council for financial support.

**Supporting Information Available:** Classical molecular dynamics of DNA and RNA duplexes, and electron and shielding density differences between A:T nucleotide and isolated base pair. This material is available free of charge via the Internet at <http://pubs.acs.org>.

JA0577903